# A Study of Boratriazaroles: An Underdeveloped Class of Heterocycles

Sean K. Liew, Aleksandra Holownia, Andrew J. Tilley, Elisa I. Carrera, Dwight S. Seferos,* and Andrei K. Yudin*

Davenport and Lash Miller Chemical Laboratories, Department of Chemistry, University of Toronto, 80 Saint George Street, Toronto, Ontario M5S 3H6, Canada

Ⓢ *Supporting Information*

ABSTRACT: Boratriazaroles were discovered in the late 1960s, and since then, a variety of substituted boratriazarole derivatives have been prepared. However, no study has compared the properties of these BN heterocycles with their carbon-based analogues. In this work, we have prepared a series of boratriazarole derivatives and have investigated how structural variations in the five-member heterocycle affect photophysical and electronic properties. Boratriazaroles exhibit absorption and emission spectra comparable to those of their azacycle analogues but have a markedly lower quantum yield. The quantum yield can be increased with the incorporation of a 2-pyridyl substitution on the boratriazaroles, and the structural and optoelectronic properties are further influenced by the nature of the B-aryl substituent. Introducing an electron-deficient *p*-cyano group on the B-phenyl substituent creates a twisted intramolecular charge transfer state that causes a large Stokes shift and positive solvatochromism. Our work should serve to guide future synthetic efforts toward the application of boratriazaroles in materials science.
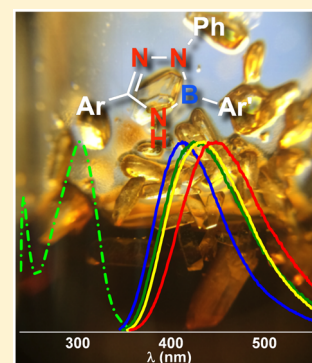
INTRODUCTION

The synthesis and study of boron-containing heterocycles has become an active area of research.[1,2] A common approach to incorporate boron into heterocycles is to substitute C=C functionality with the isosteric and isoelectronic B−N moiety.[3,4] When B−N functionality is incorporated into aromatic heterocycles, some degree of aromaticity is retained.[5] The diversity of new aromatic B−N-containing heterocycles imparts new intermolecular interactions and changes in photophysical properties, which can be exploited in areas such as optoelectronics[6−8] and drug discovery.[9]

In 1926, Stock and Pohland reported the first example of interchanging C=C with B−N with their synthesis of borazine, the BN analogue of benzene.[10] Over the past decade, many advances in the synthesis of new aromatic B−N-containing heterocycles have been achieved.[5−9,11−13,42,43] Despite the vast amount of research dedicated to exploring the ramifications of C=C to B−N substitutions, 5-member aromatic boron-containing heterocycles,[14−27] such as boratriazaroles,[28−37] have not been fully explored. Boratriazaroles are B−N isosteres of imidazoles and pyrazoles, two azacycles that are important scaffolds in the pharmaceutical and agrochemical industry,[38] and have various applications in materials science.[39−41] The first documented boratriazarole synthesis was by Paetzold, who reported only a 5% yield of the desired product.[28] In 1971, Dewar synthesized a number of boratriazaroles by treating a hydrazonamide with substituted boronic acids.[29,30] In 2015, Pitterna and co-workers investigated 3-pyridyl-containing disubstituted boratriazaroles and found that the heterocycles were stable in slightly basic solution that were in part attributed to steric bulk on the boronic acid substituent.[31] Kinjo and co-workers demonstrated the synthesis of new B−M and B−E

boratriazarole complexes (M = metal, E = C-based electrophile) derived from B-lithiated triazaboryl anions.[32,33] Our lab explored new boratriazarole-containing biaryl motifs derived from bromoacyl MIDA boronate scaffolds.[34] The resulting bisheteroaryl products exhibited excellent thermal stability and formed intermolecular hydrogen bonds in the solid state that are not possible with the C=C analogues. Despite the current interest in the synthesis and application of these heterocycles, no study has compared the physical properties of boratriazaroles to their carbon-based analogues. Herein, we report the synthesis, and photophysical and electronic properties of boratriazaroles and their analogues. Using a range of experimental and computational techniques, we show how structural variations in the five-member heterocycle and the aryl-substitution have a marked effect on the photophysical and electronic properties of boratriazaroles. This work provides fundamental new insight into the properties of boratriazaroles that will aid the design of new molecules and potential functional materials.

RESULTS

A family of trisubstituted azacycles were synthesized to investigate how varying the arrangement of boron, nitrogen, and carbon atoms in the central five-member heterocycle affects photophysical and electronic properties. The compounds of interest are trisubstituted boratriazarole **1**, triazole **2**, pyrazole **3**, and imidazoles **4** and **5** (Figure 1). Boratriazarole **1** is the parent compound of interest. Triazole **2** is the analogue of **1** where
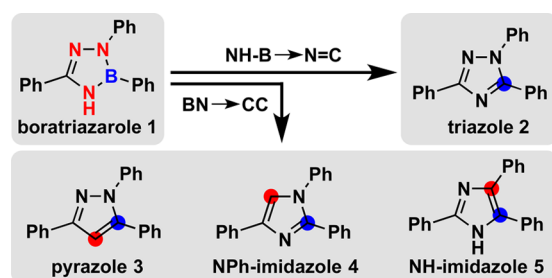
Figure 1. Analogues produced by NH-B to N=C and BN to CC swapping of boratriazarole **1**.
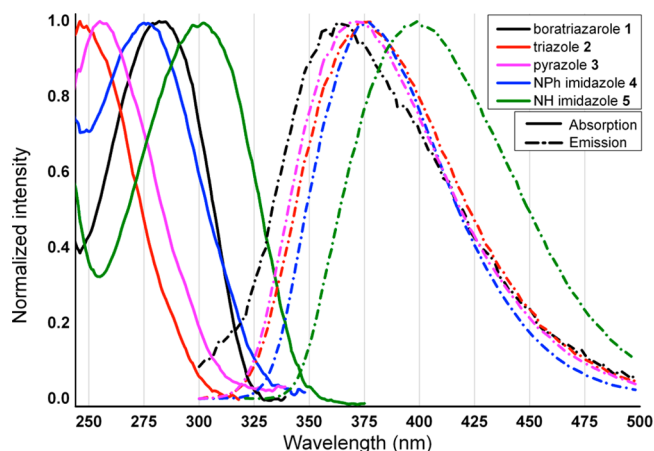

Figure 2. Normalized absorption and fluorescence emission spectra in chloroform for analogues **1–5**. An excitation wavelength of 270 nm was used for **1–4**, and 300 nm was used for **5**.

NH-B is substituted by N=C. Three other analogues, pyrazole **3** and imidazoles **4** and **5**, are variants of **2** wherein each nitrogen is systematically replaced with carbon (Figure 1).

Boratriazarole **1** was prepared from the hydrazone derived from benzaldehyde and phenyl hydrazine (Scheme 1, step a). The hydrazone was chlorinated using in situ-generated N-chlorosuccinimide dimethyl sulfide complex, and the chloride was then displaced by ammonia to afford the hydrazonamide (steps b and c). After refluxing the hydrazonamide with phenyl boronic acid, the crude product was purified by a short silica gel column followed by recrystallization in a diethyl ether/hexanes mixture to furnish **1** in 50% yield (step d). The four analogues of **1** were prepared from commercially available starting materials following literature procedures (**2–5**, Scheme 1). Briefly, the hydrazonoyl chloride precursor for **1** was also treated with benzylamine, and the resulting hydrazonamide was oxidized to furnish triazole **2** (steps e and f).[44] Pyrazole **3** was prepared in one step by treating chalcone and phenylhydrazine with molecular iodine (step g).[45] NPh-imidazole **4** was prepared by a copper-mediated coupling of the corresponding amidine with phenylacetylene (step h).[46] NH-imidazole **5** was synthesized by the acid-mediated condensation of benzil, benzaldehyde, and ammonia (step i).[47]

Optical absorption experiments were conducted in chloroform solution at room temperature to determine the photophysical properties of **1–5**. The absorption spectrum of each compound is generally broad and featureless. Boratriazarole **1** has an absorption maximum (λ_{max}) at 283 nm and a molar absorption coefficient of 2.12×10^4 M^{-1} cm^{-1} (Figure 2, Table 1)

In comparison to its analogues, the absorption spectrum of **1** is increasingly more red-shifted relative to NPh-imidazole **4**, pyrazole **3**, and triazole **2** and blue-shifted relative to NH-imidazole **5**. The red shift of **5** may be attributed to an increase in phenyl–phenyl conjugation through the C=C double bond in the imidazole. Moreover, the absorption maximum of **1** is most similar to that of NPh-imidazole **4**, differing by only 6 nm. Overall, the absorption maximum and the molar absorption coefficient of boratriazarole **1** fall within the range of its carbon-based analogues.

Using 2,5-diphenyloxazole (PPO) in cyclohexane as a standard ($\Phi_F = 0.84$),[48,49] we determined the relative fluorescence quantum yield of compounds **1–5** in chloroform. We found that NH imidazole **5** has the highest quantum yield of the series at 0.27,[50] whereas boratriazarole **1** has the lowest quantum yield of 0.01 (Table 1, $\Phi_{F(rel)}$).[25] The NH-B to N=C swapped triazole **2** has a quantum yield of 0.03 and is most similar to **1**. Although triazole **2** has a low quantum yield, it exhibits the largest Stokes shift of 13706 cm^{-1}, whereas boratriazarole **1** has the smallest Stokes shift of 7863 cm^{-1} (Table 1).

To gain insight into the electronic properties of compounds **1–5**, we performed density functional theory (DFT) calculations using Gaussian 09.[51] Time-dependent density functional

Scheme 1. Analogue syntheses[a]
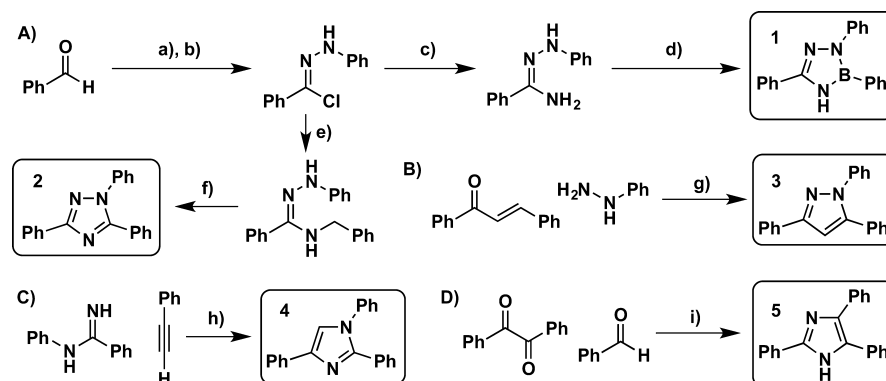
[a]Syntheses of (A) boratriazarole **1** and triazole **2** from a common precursor, (B) pyrazole **3**, (C) NPh-imidazole **4**, and (D) NH-imidazole **5**. Conditions: (a) PhNHNH₂, EtOH, 80 °C (52%); (b) N-chlorosuccinimide (NCS), SMe₂, DCM, 0 to −78 °C to rt (64%); (c) 7 N NH₃ in MeOH, rt (99%); (d) PhB(OH)₂, toluene, 100 °C (50%); (e) BnNH₂, TEA, MeCN (72%); (f) Dess–Martin periodinane (DMP), DCM, rt (62%);[44] g) I₂, 100 °C (63%);[45] (h) CuCl₂·H₂O, pyridine, Na₂CO₃, O₂, DCE, 70 °C (30%);[46] (i) NH₄OAc, AcOH, 75 °C (30%).[47]

Table 1. Summary of Photophysical and Computational Data for Analogues 1−5 Ordered by Increasing $\lambda_{max(abs)}$

	2	3	4	1	5
			experimental data		
$\lambda_{max(abs)}$ (nm)	249	255	277	283	302
$\lambda_{max(em)}$ (nm)	376	373	378	364	399
Stokes shift (cm^{-1})	13706	12406	9505	7863	8049
ε ($\times 10^4$ M^{-1}cm^{-1})	2.60	3.09	2.00	2.12	2.15
$\Phi_{F(rel)}$[a]	0.03	0.12	0.14	0.01	0.27
		computed data: B3LYP/6-311G++(d,p)//B3LYP/6-31G+(d,p)			
λ_{max} (nm)[b]	268 (0.307)	265 (0.616)	298 (0.319)	311 (0.480)	339 (0.435)
NICS (0)[c]	−7.26	−8.28	−7.98	−6.21	−7.62
NICS (1)	−7.91	−7.87	−7.11	−5.06	−6.93
NICS (−1)	−7.71	−7.53	−7.27	−4.84	−7.00

[a]Quantum yield calculated relative to PPO standard in cyclohexane $\Phi_F = 0.84$. [b]TDDFT: λ_{max} corresponding to major oscillator; oscillator strength in parentheses. [c]GIAO method.
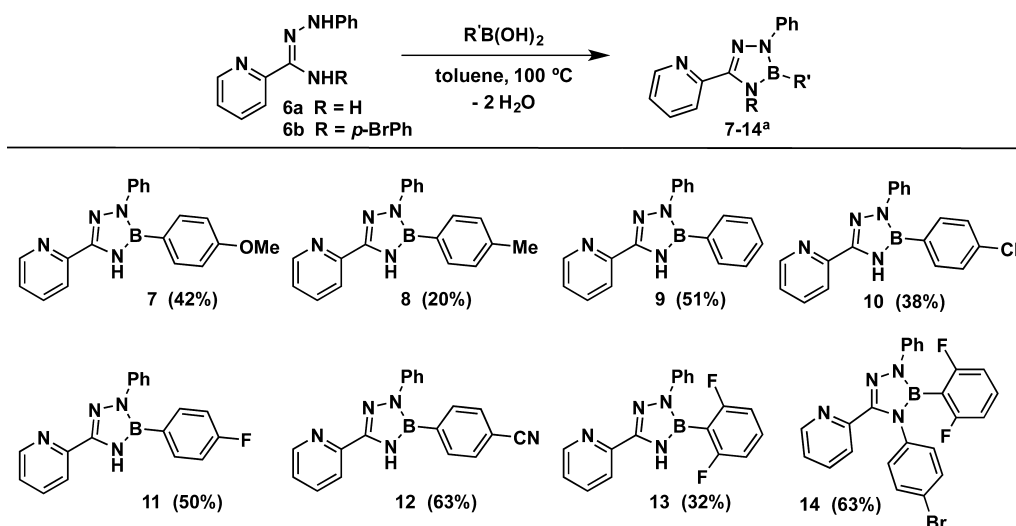

Figure 3. Boratriazarole synthesis using 2-pyridyl-substituted hydrazonamides. [a]Recrystallization yields after eluting through a plug of silica gel.

theory (TDDFT) calculations were carried out using B3LYP/6-311G++(d,p) on geometries optimized using B3LYP/6-31G+(d,p). Stationary points were analyzed using frequency calculations at 298 K. The calculations slightly overestimated the absorption λ_{max} (corresponding to the transition with the highest oscillator strength) but were consistent with the overall experimental trend (Table 1, λ_{max} computed). We also performed nucleus-independent chemical shift (NICS) calculations at the centroid (0), and one angstrom above and below the plane of the 5-member ring (NICS (1) and NICS (−1), respectively) to assess aromaticity.[52] A more negative NICS value implies higher aromatic character when comparing rings of the same size. On the basis of the obtained values, boratriazarole 1 is in fact aromatic with a NICS (0) value of −6.21, but to a lesser extent compared to 2−5 as indicated by their more negative NICS values ranging from −8.28 to −7.26 (Table 1, NICS).

Having characterized boratriazarole 1 relative to analogues 2−5, we next sought to understand how the B-aryl substituents of boratriazaroles influence the photophysical and electronic properties. In our pursuit to synthesize boratriazaroles from various hydrazonamide precursors, we found the preparation of 2-pyridyl hydrazonamides 6 to be the most efficient and scalable. The attempted synthesis of various other hydrazonoyl

chlorides using the chlorination procedures led to no reaction due to insolubility in the case of 2-naphthyl substitution, or mixtures of undesired products with 3- and 4-pyridyl substitution. We thus used 6 to prepare a small series of 2-pyridyl-substituted boratriazaroles with various aryl boronic acids. The appropriate B-aryl substituents were selected to investigate how electronic properties (7−12) and steric strain (2,6-difluoro-13 and -14) influences structural and optoelectronic properties (Figure 3).

Recrystallization of four 2-pyridyl-substituted boratriazaroles yielded crystals suitable for X-ray analysis. Electron-donating p-OMe-7 and withdrawing p-CN-12, as well as more sterically encumbered 2,6-difluorophenyl boronic acid-derived tri- and tetrasubstituted boratriazaroles 13 and 14 were analyzed. A difference in the solid-state arrangement is observed for difluoro-trisubstituted boratriazarole 13, which engages in two intermolecular hydrogen bonds with the pyridine nitrogen and the NH of the central ring in a dimeric fashion. Interestingly, crystallization of p-CN-12 led to crystals containing a 2:1 mixture of product to hydrazonamide starting material. In the crystal, one molecule of 12 is hydrogen bonded to the hydrazonamide with the same two atoms as that of 13, whereas the other molecule of 12 is not participating in any hydrogen
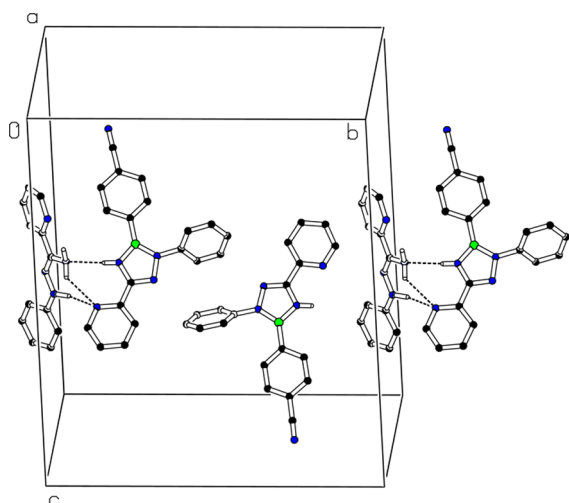
Figure 4. Unit cell of the crystal displaying two molecules of **12** and one molecule of hydrazonamide **6a**.
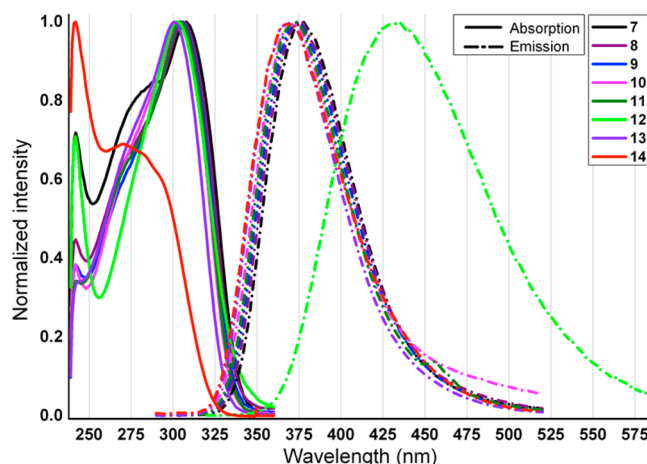

Figure 5. Normalized absorption and fluorescence emission spectra in chloroform for boratriazaroles **7−14**. An excitation wavelength of 270 nm was used for **7− 11**, **13**, and **14**, and 300 nm was used for **10**.

bonds (Figure 4).[53] Compounds **7** and **14** do not participate in hydrogen bonding in the solid state. Table 2 lists pertinent structural bond lengths and dihedral angles (see Supporting Information for additional X-ray crystallographic data).

Keeping the 2-pyridyl and *N*-phenyl groups on the boratriazarole constant allowed us to assess the role of the B-aryl substituent on photophysical properties. To this end, we recorded the optical absorption and fluorescence spectra for the six *para*-substituted boratriazaroles (**7−12**) as well as the difluorophenyl boronic acid derived tri- and tetrasubstituted boratriazaroles (**13** and **14**). The solution absorption maxima of compounds **7−13** fall between 301 and 308 nm, which we assign to the 0−0 vibronic transition (Figure 5, Table 3, $\lambda_{\text{max(abs)}}$). In contrast, tetrasubstituted **14** has an absorption maximum at 240 nm and a lower intensity band at 272 nm. Given the similar energy of this longer wavelength transition to the 0−0 vibronic band of compounds **7−13**, we tentatively assign the feature at 272 nm to the 0−0 vibronic transition. The higher energy feature at 240 nm thus presumably corresponds to a higher energy vibronic transition common to each molecule in the series. All of the molecules have molar absorption coefficients ranging from 1.51×10^4 to $2.33 \times 10^4 \text{ M}^{-1} \text{ cm}^{-1}$ with **14** having the lowest (calculated at 272 nm) and *p*-CN-**12** having the highest value (Table 3, ε). The fluorescence emission λ_{max} of all but one of the compounds occurs within a small range

from 368 to 377 nm (Figure 5, Table 3, $\lambda_{\text{max(em)}}$). The emission maximum of *p*-CN-**12** occurs at 435 nm and exhibits the largest Stokes shift of 10015 cm^{-1}. Tetrasubstituted **14** also has a large Stokes shift of 9664 cm^{-1}. Furthermore, we obtained the quantum yields for all compounds relative to PPO and found that switching the hydrazonamide-derived phenyl group of **1** to (2-pyridyl)-**9** led to a drastic increase in the quantum yield of the boratriazarole from 0.01 to 0.47 (Table 3, $\Phi_{\text{F(rel)}}$). The quantum yields of the various trisubstituted compounds do not follow a trend based on the electronic properties of the B-aryl ring ($\Phi_{\text{F}} = 0.32-0.52$). Tetrasubstituted boratriazarole **14** has a much lower quantum yield of 0.13.
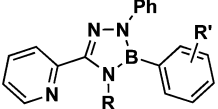
Compounds with large Stokes shifts often exhibit solvatochromic behavior.[54−56] Because *p*-CN-**12** displayed a significantly larger Stokes shift relative to that of the other compounds in the series, we investigated the solvatochromic behavior of this compound by recording the absorption and emission spectra of **12** in solvents with varying polarities. The absorption maximum of **12** varies within a small range of 297−303 nm when recorded in these solvents (Table 4). The emission maximum of **12**, however, is substantially red-shifted as the polarity of the solvent increases. In diethyl ether, the emission maximum appears at 412 nm, corresponding to a Stokes shift of 8950 cm^{-1}, and in the more polar acetonitrile, the emission maximum appears at 448 nm with a correspondingly larger

Table 2. Selected X-ray Crystallographic Data for 7 and 12−14[a]

	7	**12**[b]	**13**[b]	**14**
	R = H, R′ = *p*-OMe	R = H, R′ = *p*-CN	R = H, R′ = 2,6-F$_2$	R = *p*-BrPh, R′ = 2,6-F$_2$
B−N$_a$ (Å)	1.4300(17)	1.427(2), 1.428(2)	1.419(2), 1.416(2)	1.438(3)
B−N$_b$ (Å)	1.4312(17)	1.432(2), 1.430(2)	1.427(2), 1.434(2)	1.414(3)
ψ^1 (deg)	2.31(9)	6.77(11), 7.03(11)	10.10(9), 13.02(9)	32.05(13)
ψ^2 (deg)	72.03(4)	54.73(5), 52.66(5)	10.63(9), 13.66(9)	24.15(8)
ψ^3 (deg)	11.0(3)	11.20(10), 6.22(10)	76.62(7), 51.58(7)	56.43(9)
ψ^4 (deg)				63.59(10)

[a] ψ = dihedral angle between the two aryl rings. [b] Two values for **12** and **13** correspond to two molecules in the unit cell.

Table 3. Summary of Photophysical and Computational Data for Boratriazaroles 7−14

	R = H							R = p-BrPh
	7	8	9	10	11	12	13	14
	R′ = p-OMe	R′ = p-Me	R′ = p-H	R′ = p-Cl	R′ = p-F	R′ = p-CN	R′ = 2,6-F2	R′ = 2,6-F2
	experimental data							
$\lambda_{max(abs)}$ (nm)	308	306	305	303	305	303	301	272
$\lambda_{max(em)}$ (nm)	377	375	374	372	372	435	368	369
Stokes shift (cm^{-1})[a]	5942	6013	6049	6122	5905	10015	6049	9664
ε ($\times 10^4$ M^{-1}cm^{-1})	1.99	2.06	1.77	2.21	2.05	2.33	2.11	1.51
$\Phi_{F(rel)}$[b]	0.52	0.44	0.47	0.32	0.52	0.32	0.51	0.13
	computed data: B3LYP/6-311G++(d,p)//B3LYP/6-31G+(d,p)							
λ_{max} (nm)[c]	335 (0.334)	329 (0.369)	327 (0.377)	324 (0.391)	324 (0.377)	318 (0.377)	321 (0.373)	311 (0.179)
NICS (0)[d]	−6.52	−6.59	−6.64	−6.69	−6.69	−6.78	−6.98	−6.74
NICS (1)	−5.25	−5.26	−5.37	−5.45	−5.36	−5.46	−5.56	−5.04
NICS (−1)	−5.08	−5.15	−5.27	−5.20	−5.22	−5.30	−5.56	−5.27

[a]The Stokes shift is quoted as the difference between the 0−0 vibronic band of the solution absorption spectrum and the solution emission maximum. [b]Quantum yield calculated relative to PPO standard in cyclohexane (Φ_F = 0.84). [c]TDDFT: λ_{max} corresponding to major oscillator; oscillator strength in parentheses. [d]GIAO method.

Table 4. Absorption and Emission Maxima and Stokes Shift for 12 in Different Solvents

solvent	Et$_2$O	THF	EtOAc	CHCl$_3$	MeCN
$\lambda_{max(abs)}$ (nm)	301	302	300	303	295
$\lambda_{max(em)}$ (nm)	412	424	424	435	448
Stokes shift (cm^{-1})[a]	8950	9528	9748	10014	11576

[a]The Stokes shift is quoted as the difference between the 0−0 vibronic band of the solution absorption spectrum and the solution emission maximum.

Stokes shift of 11576 cm^{-1}. Using methanol and DMSO as solvent led to significant emission quenching compared to that of the other solvents, possibly due to sample decomposition. Nevertheless, a Stokes shift of similar magnitude to that of acetonitrile was observed for each of these polar solvents (see Supporting Information) and is consistent with positive solvatochromism.

We next conducted computational studies on the substituted boratriazaroles to further understand their electronic properties. As with analogues **1−5**, the calculated absorbance maxima were slightly overestimated but consistent with the trend of the experimental values for **7−14** (Table 3, λ_{max} computed). NICS calculations revealed that the central boratriazarole ring is relatively more aromatic with the 2-pyridyl substitution compared to **1**. Consistent with the data from the B−N bond lengths derived from the X-ray crystallographic data (vide infra), NICS calculations also show a trend of increased aromaticity with more electron-withdrawing substituents. To gain insight into the substantial Stokes shift with p-CN-**12**, the HOMO and LUMO orbitals from the TDDFT calculations were visualized. In general, p-OMe, p-Me, p-H, p-Cl, p-F, and 2,6-difluoro-substituted boratriazaroles have very similar HOMO and LUMO orbitals (Figure 6, only OMe and Cl shown, see Supporting Information for more detail). The HOMO is delocalized among the four aryl rings, and the LUMO predominates on the pyridyl ring with no contribution from the

B-aryl substituent. The introduction of the p-CN substitution drastically alters the electronic distribution in the LUMO orbital, which predominates on the B-aryl substituent. With the additional N-aryl ring in **14**, there is less delocalization in the HOMO orbital and a large contribution of the new N-aryl ring to the LUMO orbital. The transitions corresponding to the highest oscillator strengths are from the HOMO to the LUMO for all compounds except **12**. Although the HOMO to LUMO transition does contribute to the spectrum of **12** (f = 0.187), the transition with the highest oscillator strength is HOMO to LUMO+1 in nature (f = 0.377). The electronic distribution in the LUMO+1 of **12** resembles that of the LUMOs of all of the other compounds.

DISCUSSION

On the basis of our study, the boratriazaroles are less aromatic compared to that of the carbon-based analogues. This property is elucidated by the NICS calculations, whereby the NICS values for **1** are less negative than those for **2−5**. We conclude that the boratriazaroles do not exist as the formally zwitterionic RHN$^+$=B$^-$NPh species; rather, the NH lone pair in **1** is more localized on nitrogen and partially donating into the boron p-orbital. The overall aromaticity is further supported by the X-ray crystallographic data of **7** and **12−14**, which show that the central boratriazarole rings are essentially planar with root-mean-square deviations in the range of 0.004−0.006 Å. The trend of decreased aromaticity in the boratriazaroles is consistent with that in other studies of BN heterocycles.[26,27,57]

We have investigated changes in the boron−nitrogen bond lengths as well as changes in the dihedral angles between the central boratriazarole ring and its flanking aryl groups (Table 2) in the X-ray crystallographic data of the 2-pyridyl-boratriazarole analogues p-OMe-**7**, p-CN-**12**, 2,6-difluoro-**13**, and tetrasubstituted-**14**. Because N$_b$ is bound to a phenyl group, which will delocalize the nitrogen lone pair, the resulting N$_b$−B bond lengths for **7**, **12**, and **13** are longer than N$_a$−B. There is more donation of the N$_a$H lone pair into the p-orbital of boron. As
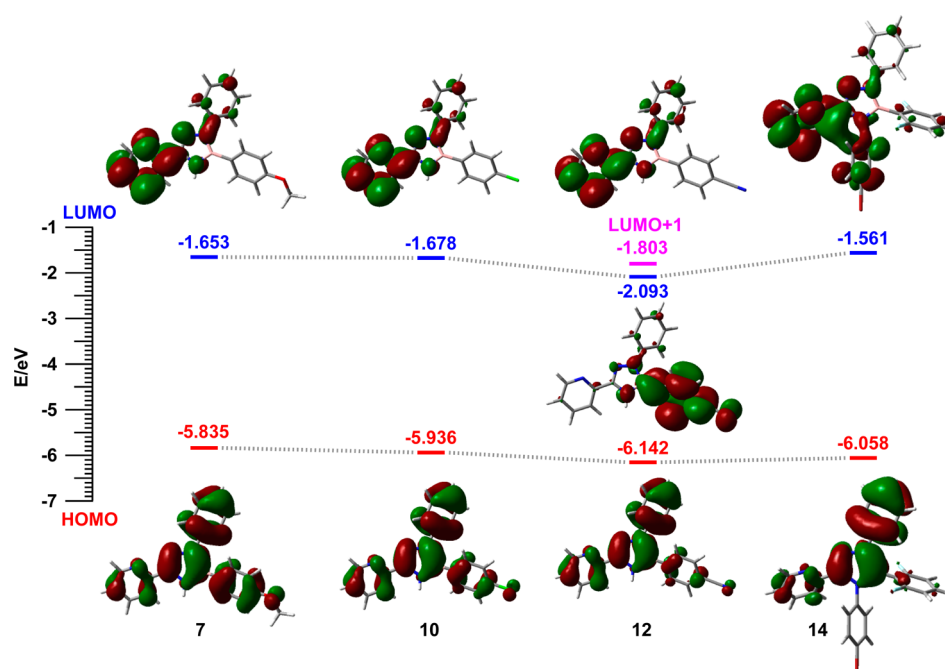
Figure 6. Computed HOMO and LUMO orbitals of *p*-OMe-**7**, Cl-**10**, and CN-**12**, and **14**.

the electron-withdrawing nature of the B-aryl substituent increases, the bond length between the boron and both nitrogen atoms decreases. By swapping the NH with N-aryl (as in **14**), the N_b−B bond becomes shorter than N_a−B, presumably due to steric repulsion between the N_a-aryl group with the pyridyl and B-aryl substituents. For each compound, all B−N bond lengths are longer than a B−N double bond (∼1.41 Å) implying electron delocalization in the aromatic system.[58]

Steric repulsion was also assessed by the dihedral angles between the central boratriazarole ring and its flanking aryl rings. For **7** and **12**, the N_b-phenyl ring (ψ^2) is twisted the most out of plane at 72° and ∼53°, respectively, whereas the pyridyl $(\psi^1 < 7°)$ and B-aryl $(\psi^3 < 12°)$ are nearly in plane with the central ring. In contrast, bulkier difluoro-**13** has the B-aryl group twisted approximately 64° out of plane, whereas the pyridyl and phenyl groups are more in plane $(\psi^{1,2} < 14°)$. Once an aryl substituent is introduced on N_a as with **14**, all dihedral angles increase, thus decreasing electronic communication among the π-systems and affecting the absorption properties.

With the exception of NH-imidazole **5**, the boratriazaroles contain a hydrogen bond donor NH that is absent from the other analogues. In our previous studies of boratriazaroles, we observed that the NH functionality is capable of engaging in intermolecular hydrogen bonding interactions in the solid state.[34] Hydrogen bonding capabilities were also further elucidated in the solid state of the (2-pyridyl)boratriazaroles. Only difluoro-**13** was capable of participating in intermolecular hydrogen bonding in a dimeric fashion. The other observed case of hydrogen bonding was with *p*-CN-**12**, which was unable to pack in a dimeric fashion but cocrystallized with the hydrazonamide starting material (vide supra, Figure 4). Because the dihedral angle ψ^3 of **13** is high (>50°) due to the difluoro substitution, the compound is able to accommodate hydrogen-bond donor/acceptor interactions with a second molecule of **13** with minimal steric penalty. On the other hand, ψ^3 of **12** is much lower (<12°) with increased electronic communication between the two aryl rings, which renders dimerization in the solid state sterically inaccessible. The cocrystallized hydrazona-

mide can be oriented to minimize steric repulsion and favorably hydrogen bond with the boratriazarole (see Supporting Information for X-ray crystallographic data). The unusual cocrystallization of the product with residual starting material may speak to the high propensity of these pyridyl boratriazaroles to participate in hydrogen bonding, which is a desirable property for applications in medicinal chemistry.

Relative to the carbon-based analogues (**2**−**5**), boratriazarole **1** generally has similar absorption and emission spectra, but has a very low quantum yield. The quantum yield, however, can be increased with the inclusion of a pyridyl group in the molecule. A number of conclusions can be drawn from the photophysical data as well as the TDDFT calculations and molecular orbital diagrams for the HOMO and LUMO of **7**−**14**. With trisubstituted boratriazaroles **7**−**13**, the HOMO is delocalized across the entire molecule. With the exception of *p*-CN-**12**, the main computed transition contributing to the absorption spectrum is a HOMO to LUMO π−π* transition with some charge transfer character away from the B-aryl ring onto the pyridyl ring. When donor and acceptor units are connected through a single bond, such charge-transfer behavior is accompanied by a change in geometry to establish a lower-energy twisted intramolecular charge-transfer state (TICT).[59] This lower energy TICT state is observed in the emission spectrum as a significant Stokes shift. The main computed transition in **12** also involves similar charge-transfer behavior away from the B-aryl group; however, in this case, the transition occurs from HOMO to LUMO+1. A second lower intensity but significant transition for **12** is from the HOMO to LUMO, which exhibits a nearly complete charge transfer onto the B-aryl ring (Figure 6). Thus, compound **12** exhibits a significantly larger Stokes shift than the other compounds. This phenomenon is further supported by the positive solvatochromism observed for compound **12**, as excited states with strong charge-transfer character are greatly stabilized by polar solvents. Finally, the nearly complete transfer of electron density to the B-aryl ring in the LUMO likely yields a more highly twisted TICT structure than the other compounds,

which is reflected in the dramatically decreased quantum yield of emission.

■ CONCLUSIONS

We have synthesized a family of substituted boratriazaroles and have studied their photophysical and structural properties. Three BN to CC isosteres were prepared along with one NH-B to N=C substituted analogue. The boratriazaroles are aromatic, but to a lesser extent compared to that of imidazole, triazole, and pyrazole scaffolds. The quantum yield of the model triphenyl-boratriazarole is significantly lower than those of the carbon-based analogues but is shown to significantly improve upon substitution of one phenyl group with a 2-pyridyl group. This observation showcases the potential to tune photophysical properties of boratriazaroles. We subsequently analyzed the electronic and steric influence of the B-aryl ring on the photophysical properties. Although there was not a strong trend between the electronic properties of the B-aryl ring and the quantum yield, the overall aromaticity of the central boratriazarole ring is increased with electron-withdrawing groups. For the most part, the absorption and emission spectra (as well as the HOMO and LUMO levels) are not greatly influenced by the electronic properties of the B-aryl ring. The p-CN derivative is the exception to this trend, which has a large bathochromic shift relative to that of the other compounds and displays positive solvatochromic behavior. These data reveal that the boron atom in underexplored boratriazaroles is participating in electronic communication in the excited state. Judicious choice of the B-aryl substituents (such as the p-CN derivative disclosed here) can be used to tune the photophysical properties, adding further understanding to the influence and behavior of boron-containing heterocycles in polyaromatic systems. In conjunction with these findings, the use of computational tools to assess the photophysical properties of various substituted boratriazaroles is expected to aid in the development of new and improved materials.

■ EXPERIMENTAL SECTION

2,3,5-Triphenyl-2,3-dihydro-1H-1,2,4,3-triazaborole (1). Benzaldehyde (2.0 mL, 19.6 mmol) was dissolved in 95% ethanol (20 mL) and heated to 75 °C. Phenylhydrazine (10.3 mL, 104.8 mmol) was added dropwise, and the reaction was stirred for 1 h. The reaction was allowed to cool to room temperature with sustained stirring as the product crystallized out of solution. The flask was placed in a freezer for 2 h, and the product was filtered, washed with cold ethanol, and dried under high vacuum to yield (E)-1-benzylidene-2-phenyl-hydrazine (2.01 g, 52%, white crystals).[60] Hydrazonoyl chloride was prepared following literature procedures with consistent spectral data.[44,61] NCS (12.40 g, 92.9 mmol) was dissolved in anhydrous DCM (128 mL) and cooled to 0 °C. Dimethylsulfide (13.8 mL, 188.0 mmol) was added over 15 min. After stirring for an additional 15 min, the reaction was cooled to −78 °C, and the hydrazone (6.08 g, 31.0 mmol) dissolved in anhydrous DCM (100 mL) was added dropwise, allowed to stir at that temperature for 1 h, and warmed to room temperature over 3 h. The reaction was quenched with water (20 mL). Ethyl acetate was added, and the organic layer was washed with water, brine, saturated sodium sulfite solution, then water and then dried over magnesium sulfate. The solution was filtered and slowly concentrated. The product precipitated or crystallized out of solution during concentration and was filtered to yield pure product. This process could be repeated to yield multiple crops of product (Z)-N-phenylbenzohydrazonoyl chloride (4.58 g, 64%, tan solid). The hydrazonoyl chloride (1.50 g, 6.50 mmol) was dissolved in a minimum amount of methanol, and 7 N ammonia in methanol (9.3 mL, 65.0 mmol) was added dropwise and stirred for 4 h. The volatiles were

removed in vacuo, and the residue was dissolved in ethyl acetate and washed with water and brine and dried over sodium sulfate. The red solution was evaporated, and the product was purified by column chromatography with a gradient of 100% hexanes to 40% ethyl acetate in hexanes to yield (Z)-N'-phenylbenzohydrazonamide as a red oil that crystallized over time; the product turned black and may have decomposed over time (0.766 g, 56%). Mp: 65−70 °C. ¹H NMR (500 MHz, CDCl₃) δ 7.84−7.72 (m, 2H), 7.44−7.38 (m, 3H), 7.30−7.22 (m, 2H), 7.12−7.04 (m, 2H), 6.92−6.83 (m, 1H), 4.83 (br s, 2H). ¹³C NMR (126 MHz, CDCl₃) δ 151.3, 147.8, 134.1, 129.9, 129.2, 128.7, 127.5, 125.9, 120.3, 114.5. IR (neat) $\tilde{\nu}$ (cm⁻¹): 3457, 3357, 2928, 1606, 1489, 1384, 824, 750.

Hydrazonamide (0.20 g, 0.95 mmol) and phenyl boronic acid (0.12 g, 0.95 mmol) were dissolved in toluene (3.2 mL). The vessel was sealed and heated with vigorous stirring to 100 °C for 5 h. The solution was loaded onto a plug of silica gel packed with toluene, and the product was eluted with toluene. The solvent was removed in vacuo and dried thoroughly under high vacuum. The residue was dissolved in a minimum amount of diethyl ether and layered with hexanes to yield pale yellow feather-like crystals of **1** (0.144 mg, 50%). Mp: 136−138 °C (Et₂O/hexanes). ¹H NMR (500 MHz, CDCl₃) δ 7.92−7.84 (m, 2H), 7.63−7.59 (m, 2H), 7.56−7.52 (m, 2H), 7.51 (br s, 1H), 7.49−7.45 (m, 2H), 7.44−7.40 (m, 2H), 7.40−7.37 (m, 2H), 7.35−7.30 (m, 2H), 7.19−7.13 (m, 1H). ¹³C NMR (126 MHz, CDCl₃) δ 149.0, 143.7, 133.6, 129.9, 129.5, 129.4, 129.0, 128.9, 128.3, 125.5, 124.8, 122.1. ¹¹B NMR (192 MHz, CDCl₃) δ 28.0. IR (neat) $\tilde{\nu}$ (cm⁻¹): 3264, 2927, 1600, 1498, 1349, 1069, 824, 783. HRMS (DART) m/z: [M + H]⁺ calcd for C₁₉H₁₇BN₃ 298.1516, found 298.1517.

1,3,5-Triphenyl-1H-1,2,4-triazole (2). Product **2** was synthesized according to a modified literature procedure[44] and was consistent with reported spectral data.[62] Hydrazonoyl chloride (0.50 g, 2.17 mmol) was dissolved in DCM (2.2 mL) followed by the addition of benzylamine (0.71 mL, 6.5 mmol) and triethylamine (0.45 mL, 3.25 mmol) and stirred for 12 h. The DCM solution was washed with water and then brine and dried over magnesium sulfate. The product was eluted through a plug of silica using a gradient from 100% hexanes to 50% ethyl acetate in hexanes to yield (Z)-N-benzyl-N′-phenyl-benzohydrazonamide as an orange oil (0.473 g, 72%) that was used immediately in the next step. The hydrazonamide (0.30 g, 1.00 mmol) was dissolved in DCM (10 mL), and Dess−Martin periodinane (0.64 g, 1.50 mmol) was added portionwise. The solution was stirred for 5 h, then washed with saturated sodium bicarbonate solution and brine, and dried over magnesium sulfate. The orange/red crude product was purified by column chromatography with a gradient from hexanes to 25% ethyl acetate in hexanes to yield **2** as an off-white solid (0.183 g, 62%).

1,3,5-Triphenyl-1H-pyrazole (3). Product **3** was synthesized according to a modified literature procedure[45] and was consistent with reported spectral data.[63] Phenylhydrazine (0.71 mL, 7.20 mmol) and iodine (1.83 g, 7.24 mmol) were dissolved in ethanol (120 mL), and chalcone (0.50 g, 2.40 mmol) was added. The reaction was heated to 100 °C overnight. The ethanol was evaporated, and the product was redissolved in ethyl acetate, washed with saturated sodium sulfite solution and brine, and then dried over sodium sulfate. The product was first purified by column chromatography with a gradient from 100% hexanes to 10% ethyl acetate in hexanes and then recrystallized with diethyl ether/hexanes to yield **3** as a light yellow solid (0.448 g, 63%).

1,2,4-Triphenyl-1H-imidazole (4). Product **4** was prepared using a literature procedure and was consistent with reported spectral data.[46] Scale: 2.5 mmol. Pale yellow solid (0.225 g, 30%).

2,4,5-Triphenyl-1H-imidazole (5). Product **5** was prepared using a literature procedure[47] and was consistent with reported spectral data.[64] Scale: 5.0 mmol. White solid (0.444 g, 30%).

Synthesis of Hydrazonamides (Z)-N′Phenylpicolinohydrazonamide (6a) and (Z)-N-(4-Bromophenyl)-N′-phenylpicolinohydrazonamide (6b). 2-Pyridine carboxaldehyde (10 mL, 105.0 mmol) was dissolved in 95% ethanol (100 mL) and heated to 75 °C. Phenylhydrazine (10.3 mL, 105.0 mmol) was added dropwise, and the reaction was

stirred for 1 h. The reaction was allowed to cool to room temperature with sustained stirring, and the product crystallized out of solution. The flask was placed in a freezer for 2 h, and the product was filtered, washed with cold ethanol, and dried under high vacuum to yield (E)-2-((2-phenylhydrazono)methyl)pyridine (13.60 g, 66%, white crystals).[65] The hydrazone (5.00 g, 25.3 mmol) was dissolved in a minimum amount of DMF, and NCS (3.58 g, 26.8 mmol) was added portionwise over 20 min and stirred for 1 h. Water (two volume equivalents) was added dropwise, and the product precipitated out of solution. The solution was filtered, and the filter cake was washed thoroughly with water and dried under high vacuum to yield (Z)-N-phenylpicolinohydrazonoyl chloride (4.79 g, 82%, amorphous red solid). Mp: 125−127 °C. ^{1}H NMR (500 MHz, CDCl$_3$) δ 8.67 (ddd, J = 4.9, 1.8, 0.9 Hz, 1H), 8.28 (s, 1H), 8.08 (dt, J = 8.1, 1.1 Hz, 1H), 7.73 (ddd, J = 8.1, 7.4, 1.7 Hz, 1H), 7.37−7.30 (m, 2H), 7.27 (ddd, J = 7.4, 4.9, 1.1 Hz, 1H), 7.24−7.19 (m, 2H), 6.98 (tt, J = 7.4, 1.1 Hz, 1H). ^{13}C NMR (126 MHz, CDCl$_3$) δ 151.5, 149.3, 143.0, 136.4, 129.6, 125.3, 123.6, 121.9, 121.3, 113.8. IR (neat) $\tilde{\nu}$ (cm^{-1}): 3147, 2936, 1600, 1493, 1236, 1135, 845, 783. HRMS (DART) m/z: [M + H]$^+$ calcd for C$_{12}$H$_{11}$ClN$_3$ 232.0642, found 232.0642.

Synthesis of 6a. The hydrazonoyl chloride (2.00 g, 8.63 mmol) was dissolved in methanol (10 mL), and 7 N ammonia in methanol (9.9 mL, 69.1 mmol) was added dropwise and stirred for 4 h. The solvent was evaporated, and the residue was dissolved in ethyl acetate. The organic layer was washed two times with water, followed by a brine wash, and then dried over sodium sulfate. The volatiles were removed in vacuo, and the resulting red oil was dried under high vacuum and crystallized over multiple days (1.79 g, 98%, red crystals). Mp: 51−55 °C. ^{1}H NMR (500 MHz, CDCl$_3$) δ 8.53 (ddd, J = 4.9, 1.7, 1.0 Hz, 1H), 8.27 (dt, J = 8.1, 1.1 Hz, 1H), 7.72 (ddd, J = 8.1, 7.4, 1.7 Hz, 1H), 7.33−7.26 (m, 3H), 7.20−7.13 (m, 2H), 6.89 (t, J = 7.3 Hz, 1H), 6.43 (s, 1H), 5.36 (s, 2H). ^{13}C NMR (126 MHz, CDCl$_3$) δ 150.7, 148.1, 147.1, 146.1, 136.5, 129.3, 129.1, 124.0, 121.0, 120.4, 114.2. IR (neat) $\tilde{\nu}$ (cm^{-1}): 3423, 3330, 3051, 1587, 1495, 1247, 881, 788. HRMS (DART) m/z: [M + H]$^+$ calcd for C$_{12}$H$_{13}$N$_4$ 213.1140, found 213.1139.

Synthesis of 6b. The hydrazonoyl chloride (0.20 g, 0.86 mmol) and p-bromoaniline (0.22 g, 1.29 mmol) were dissolved in THF (2.9 mL), and triethylamine (0.30 mL, 2.16 mmol) was added. The solution was stirred for 2 days until complete by TLC. The volatiles were evaporated, and the residue was dissolved in ethyl acetate and washed with water and brine and then dried over sodium sulfate. The product was purified by column chromatography with a gradient from hexanes to 25% ethyl acetate in hexanes to yield an orange-yellow solid (0.274 g, 87%). Mp: 140−143 °C. ^{1}H NMR (500 MHz, CDCl$_3$) δ 8.48 (ddd, J = 4.9, 1.7, 1.0 Hz, 1H), 8.30 (dt, J = 8.1, 1.1 Hz, 1H), 7.77−7.70 (m, 2H), 7.39−7.35 (m, 2H), 7.29−7.25 (m, 2H), 7.23 (ddd, J = 7.4, 4.9, 1.2 Hz, 1H), 7.12−7.08 (m, 2H), 7.06 (br s, 1H), 6.88 (tt, J = 7.4, 1.1 Hz, 1H), 6.72−6.67 (m, 2H). ^{13}C NMR (126 MHz, CDCl$_3$) δ 152.1, 148.1, 144.5, 139.2, 136.6, 135.2, 132.1, 129.4, 123.2, 120.6, 120.1, 120.0, 114.1, 113.2. IR (neat) $\tilde{\nu}$ (cm^{-1}): 3335, 2929, 1599, 1489, 1069, 878, 783. HRMS (DART) m/z: [M + H]$^+$ calcd for C$_{18}$H$_{16}$BrN$_4$ 367.0558, found 367.0559.

General Procedure for the Synthesis of Boratriazaroles. Hydrazonamide (1 equiv) and boronic acid (1 equiv) were dissolved in toluene (0.3 M). The reaction mixture was heated to 100 °C and stirred for 6−12 h until completion, as indicated by TLC analysis. Upon completion, the reaction mixture was cooled to room temperature, loaded directly onto a silica gel plug, and eluted with toluene. The toluene was removed in vacuo, and the product was subsequently recrystallized in diethyl ether layered with hexanes to afford pure product.

2-(3-(4-Methoxyphenyl)-2-phenyl-3,4-dihydro-2H-1,2,4,3-triazaborol-5-yl)pyridine (7). Scale: 0.9 mmol. Recrystallized in Et$_2$O to yield clear, colorless crystals (126 mg, 42%). Mp: 110−112 °C. ^{1}H NMR (400 MHz, CDCl$_3$) δ 8.60 (ddd, J = 4.9, 1.7, 1.0 Hz, 1H), 8.52 (s, 1H), 8.21 (dt, J = 8.0, 1.1 Hz, 1H), 7.81−7.72 (m, 1H), 7.62−7.49 (m, 4H), 7.39−7.32 (m, 2H), 7.29 (ddd, J = 7.5, 4.9, 1.2 Hz, 1H), 7.19 (ddt, J = 8.6, 6.9, 1.2 Hz, 1H), 6.95−6.87 (m, 2H), 3.84 (s, 3H). ^{13}C NMR (126 MHz, CDCl$_3$) δ 160.8, 149.3, 149.0, 148.1, 143.9, 136.8, 135.3, 129.0, 125.1, 123.7, 122.7, 120.4, 113.9, 55.2. ^{11}B NMR

(128 MHz, CDCl$_3$) δ 27.7. IR (neat) $\tilde{\nu}$ (cm^{-1}): 3460, 3056, 2932, 1599, 1498, 1453, 1412, 1346, 1396, 1243. HRMS (DART) m/z: [M + H]$^+$ calcd for C$_{19}$H$_{17}$BN$_4$O 329.1574, found 329.1569.

2-(2-Phenyl-3-(p-tolyl)-3,4-dihydro-2H-1,2,4,3-triazaborol-5-yl)pyridine (8). Scale: 0.9 mmol. Recrystallized in Et$_2$O/hexanes to yield clear, colorless crystals (58 mg, 20%). Mp: 105−108 °C. ^{1}H NMR (400 MHz, CDCl$_3$) δ 8.60 (dt, J = 5.1, 1.4 Hz, 1H), 8.54 (s, 1H), 8.22 (dt, J = 8.0, 1.1 Hz, 1H), 7.77 (td, J = 7.8, 1.7 Hz, 1H), 7.58−7.49 (m, 4H), 7.37−7.32 (m, 2H), 7.29 (ddd, J = 7.5, 4.9, 1.2 Hz, 1H), 7.21−7.15 (m, 3H), 2.38 (s, 3H). ^{13}C NMR (126 MHz, CDCl$_3$) δ 149.3, 149.0, 148.1, 143.8, 139.5, 136.8, 133.8, 129.0, 129.0, 125.1, 123.8, 122.6, 120.4, 21.7. ^{11}B NMR (128 MHz, CDCl$_3$) δ 27.8. IR (neat) $\tilde{\nu}$ (cm^{-1}): 3465, 3054, 2923, 1592, 1479, 1459, 1410, 1346, 806, 766. HRMS (DART) m/z: [M + H]$^+$ calcd for C$_{19}$H$_{17}$BN$_4$ 313.1625, found 313.1617.

2-(2,3-Diphenyl-3,4-dihydro-2H-1,2,4,3-triazaborol-5-yl)pyridine (9). Scale: 0.9 mmol. Recrystallized in Et$_2$O/hexanes to yield clear, orange crystals (135 mg, 51%). Mp: 76−78 °C. ^{1}H NMR (400 MHz, CDCl$_3$) δ 8.60 (ddd, J = 4.9, 1.8, 1.0 Hz, 1H), 8.58 (br s, 1H), 8.23 (dt, J = 8.0, 1.1 Hz, 1H), 7.77 (td, J = 7.7, 1.7 Hz, 1H), 7.65−7.59 (m, 2H), 7.58−7.52 (m, 2H), 7.44−7.32 (m, 5H), 7.30 (ddd, J = 7.5, 4.9, 1.2 Hz, 1H), 7.22−7.15 (m, 1H). ^{13}C NMR (126 MHz, CDCl$_3$) δ 149.3, 149.1, 148.1, 143.7, 136.8, 133.7, 129.5, 129.0, 128.2, 125.1, 123.8, 122.6, 120.4. ^{11}B NMR (128 MHz, CDCl$_3$) δ 28.0. IR (neat) $\tilde{\nu}$ (cm^{-1}): 3231, 2959, 1596, 1494, 1418, 1340, 752, 702. HRMS (DART) m/z: [M + H]$^+$ calcd for C$_{18}$H$_{15}$BN$_4$ 299.1468, found 299.1471.

2-(3-(4-Chlorophenyl)-2-phenyl-3,4-dihydro-2H-1,2,4,3-triazaborol-5-yl)pyridine (10). Scale: 0.47 mmol. Recrystallized in Et$_2$O to yield clear, orange crystals (59.9 mg, 38%). Mp: 111−114 °C. ^{1}H NMR (500 MHz, CDCl$_3$) δ 8.60 (ddd, J = 4.9, 1.7, 1.0 Hz, 1H), 8.59 (s, 1H), 8.21 (dt, J = 8.0, 1.1 Hz, 1H), 7.77 (ddd, J = 8.0, 7.5, 1.7 Hz, 1H), 7.57−7.52 (m, 2H), 7.52−7.48 (m, 2H), 7.41−7.32 (m, 4H), 7.30 (ddd, J = 7.5, 4.9, 1.2 Hz, 1H), 7.24−7.16 (m, 1H). ^{13}C NMR (126 MHz, CDCl$_3$) δ 149.4, 149.1, 147.9, 143.5, 136.9, 135.8, 135.1, 129.1, 128.5, 125.4, 123.9, 122.6, 120.4. ^{11}B NMR (160 MHz, CDCl$_3$) δ 27.2. IR (neat) $\tilde{\nu}$ (cm^{-1}): 3456, 3057, 1590, 1474, 1343, 1284, 1083, 813, 781. HRMS (DART) m/z: [M + H]$^+$ calcd for C$_{18}$H$_{15}$BClN$_4$ 333.1078, found 333.1082.

2-(3-(4-Fluorophenyl)-2-phenyl-3,4-dihydro-2H-1,2,4,3-triazaborol-5-yl)pyridine (11). Scale: 0.9 mmol. Recrystallized in 1:1 DCM/hexanes to yield clear, orange crystals (147 mg, 50%). Mp: 112−115 °C. ^{1}H NMR (400 MHz, CDCl$_3$) δ 8.60 (ddd, J = 4.9, 1.8, 1.0 Hz, 1H), 8.56 (br s, 1H), 8.21 (dt, J = 8.0, 1.1 Hz, 1H), 7.77 (ddd, J = 8.0, 7.5, 1.7 Hz, 1H), 7.63−7.55 (m, 2H), 7.54−7.47 (m, 2H), 7.38−7.32 (m, 2H), 7.30 (ddd, J = 7.5, 4.9, 1.2 Hz, 1H), 7.20 (ddt, J = 7.9, 6.9, 1.2 Hz, 1H), 7.12−7.00 (m, 2H). ^{13}C NMR (126 MHz, CDCl$_3$) δ 163.9 (d, J = 248.9 Hz), 149.3, 149.1, 148.0, 143.6, 136.9, 135.7 (d, J = 7.7 Hz), 129.1, 125.3, 123.9, 122.7, 120.4, 115.4 (d, J = 20.1 Hz). ^{11}B NMR (128 MHz, CDCl$_3$) δ 27.7. ^{19}F NMR (377 MHz, CDCl$_3$) δ −110.9. IR (neat) $\tilde{\nu}$ (cm^{-1}): 3451, 3054, 1596, 1496, 1413, 1342, 1214, 837, 767. HRMS (DART) m/z: [M + H]$^+$ calcd for C$_{18}$H$_{14}$BFN$_4$ 317.1374, found 317.1376.

4-(2-Phenyl-5-(pyridin-2-yl)-2,4-dihydro-3H-1,2,4,3-triazaborol-3-yl)benzonitrile (12). Scale: 0.47 mmol. Recrystallized in Et$_2$O to yield clear, pale orange crystals (96.3 mg, 63%). Mp: 126−128 °C. ^{1}H NMR (500 MHz, CDCl$_3$) δ 8.70 (br s, 1H), 8.60 (ddd, J = 4.9, 1.7, 1.0 Hz, 1H), 8.22 (dt, J = 8.0, 1.1 Hz, 1H), 7.79 (ddd, J = 8.0, 7.5, 1.7 Hz, 1H), 7.73−7.68 (m, 2H), 7.67−7.61 (m, 2H), 7.50−7.43 (m, 2H), 7.40−7.34 (m, 2H), 7.32 (ddd, J = 7.5, 4.9, 1.2 Hz, 1H), 7.25−7.21 (m, 1H). ^{13}C NMR (126 MHz, CDCl$_3$) δ 149.6, 149.1, 147.7, 143.1, 137.0, 134.2, 131.6, 129.2, 125.7, 124.1, 122.7, 120.4, 119.0, 113.1. ^{11}B NMR (160 MHz, CDCl$_3$) δ 26.9. IR (neat) $\tilde{\nu}$ (cm^{-1}): 3272, 2927, 2166, 1600, 1494, 1341, 1091, 832, 765. HRMS (DART) m/z: [M + H]$^+$ calcd for C$_{19}$H$_{15}$BN$_5$ 324.1421, found 324.1430.

2-(3-(2,6-Difluorophenyl)-2-phenyl-3,4-dihydro-2H-1,2,4,3-triazaborol-5-yl)pyridine (13). Scale: 0.471 mmol. Recrystallized in Et$_2$O/hexanes to yield clear, off-white crystals (50 mg, 32%). Mp: 110−113 °C. ^{1}H NMR (500 MHz, CDCl$_3$) δ 8.76 (s, 1H), 8.60 (ddd, J = 4.9, 1.8, 1.0 Hz, 1H), 8.24 (dt, J = 8.0, 1.1 Hz, 1H), 7.78 (ddd, J = 8.0,

7.5, 1.7 Hz, 1H), 7.52−7.45 (m, 2H), 7.41 (tt, J = 8.3, 6.7 Hz, 1H), 7.35−7.28 (m, 3H), 7.21−7.13 (m, 1H), 6.99−6.85 (m, 2H). ^{13}C NMR (126 MHz, CDCl$_3$) δ 165.3 (dd, J = 247.3, 12.6 Hz), 149.8, 149.1, 147.8, 143.8, 136.9, 132.5 (t, J = 10.3 Hz), 128.9, 125.0, 123.9, 121.1, 120.4, 112.4−110.7 (m). ^{11}B NMR (160 MHz, CDCl$_3$) δ 24.5. ^{19}F NMR (376 MHz, CDCl$_3$) δ −99.9. IR (neat) $\tilde{\nu}$ (cm^{-1}): 3234, 2928, 1596, 1500, 1343, 1227, 1118, 1105, 982, 785. HRMS (DART) m/z: [M + H]$^+$ calcd for C$_{18}$H$_{14}$BF$_2$N$_4$ 335.1280, found 335.1286.

2-(4-(4-Bromophenyl)-3-(2,6-difluorophenyl)-2-phenyl-3,4-dihydro-2H-1,2,4,3-triazaborol-5-yl)pyridine (14). Scale: 0.272 mmol. Recrystallized in Et$_2$O/hexanes to yield clear, pale yellow crystals (83.3 mg, 63%). Mp: 160−163 °C. ^{1}H NMR (500 MHz, CDCl$_3$) δ 8.43 (ddd, J = 4.8, 1.8, 1.0 Hz, 1H), 7.80 (dt, J = 7.9, 1.1 Hz, 1H), 7.71 (ddd, J = 7.6, 1.8 Hz, 1H), 7.49−7.44 (m, 2H), 7.35 (ddd, J = 8.3, 6.8, 1.6 Hz, 1H), 7.31−7.26 (m, 4H), 7.22 (ddd, J = 7.6, 4.8, 1.2 Hz, 1H), 7.16−7.11 (m, 1H). ^{13}C NMR (126 MHz, CDCl$_3$) δ 164.8 (dd, J = 245.8, 12.5 Hz), 149.4, 149.3, 148.7, 142.9, 138.6, 136.6, 132.7 (t, J = 10.1 Hz), 131.8, 129.1, 128.2, 125.2, 124.3, 123.6, 120.7, 120.1, 111.7−111.1 (m). ^{11}B NMR (160 MHz, CDCl$_3$) δ 25.7. ^{19}F NMR (470 MHz, CDCl$_3$) δ −99.9. IR (neat) $\tilde{\nu}$ (cm^{-1}): 2927, 1621, 1489, 1381, 1350, 1258, 1228, 1066, 834, 788. HRMS (DART) m/z: [M + H]$^+$ calcd for C$_{24}$H$_{17}$BBrF$_2$N$_4$ 489.0698, found 489.0705.

■ ASSOCIATED CONTENT

Ⓢ Supporting Information

The Supporting Information is available free of charge on the ACS Publications website at DOI: 10.1021/acs.joc.6b01565.

> Computational data, X-ray crystallographic data, and ^{1}H, ^{13}C, ^{11}B, ^{19}F NMR spectra (PDF)
>
> X-ray crystallographic data for **7** (CCDC 1485646) (CIF)
> X-ray crystallographic data for **12** (CCDC 1485647) (CIF)
> X-ray crystallographic data for **13** (CCDC 1485644) (CIF)
> X-ray crystallographic data for **14** (CCDC 1485645) (CIF)

■ AUTHOR INFORMATION

Corresponding Authors
*E-mail: dseferos@chem.utoronto.ca.
*E-mail: ayudin@chem.utoronto.ca.

Notes
The authors declare no competing financial interest.

■ ACKNOWLEDGMENTS

■ REFERENCES

(1) Review: Wang, B. J.; Groziak, M. P. *Adv. Heterocycl. Chem.* **2016**, *118*, 47−90 and references therein.
(2) *Synthesis and Application of Organoboron Compounds*; Fernández, E., Whiting, A., Eds.; Springer: New York, 2015.
(3) Liu, Z.; Marder, T. B. *Angew. Chem., Int. Ed.* **2008**, *47*, 242−244.
(4) Review: Bosdet, M. J. D.; Piers, W. E. *Can. J. Chem.* **2009**, *87*, 8−29 and references therein.
(5) Review: Campbell, P. G.; Marwitz, A. J. V.; Liu, S.-Y. *Angew. Chem., Int. Ed.* **2012**, *51*, 6074−6092 and references therein.
(6) Bosdet, M. J. D.; Jaska, C. A.; Piers, W. E.; Sorensen, T. S.; Parvez, M. *Org. Lett.* **2007**, *9*, 1395−1398.
(7) Jaska, C. A.; Piers, W. E.; McDonald, R.; Parvez, M. *J. Org. Chem.* **2007**, *72*, 5234−5243.
(8) Baggett, A. W.; Guo, F.; Li, B.; Liu, S.-Y.; Jäkle, F. *Angew. Chem., Int. Ed.* **2015**, *54*, 11191−11195.
(9) Liu, L.; Marwitz, A. J. V.; Matthews, B. W.; Liu, S.-Y. *Angew. Chem., Int. Ed.* **2009**, *48*, 6817−6819.
(10) Stock, A.; Pohland, E. *Chem. Ber.* **1926**, *59*, 2215−2223.
(11) Ruman, T.; Jarmuła, A.; Rode, W. *Bioorg. Chem.* **2010**, *38*, 242−245.
(12) Shi, Y.-G.; Yang, D.-T.; Mellerup, S. K.; Wang, N.; Peng, T.; Wang, S. *Org. Lett.* **2016**, *18*, 1626−1629.
(13) Huang, H.; Pan, Z.; Cui, C. *Chem. Commun.* **2016**, *52*, 4227−4230.
(14) Ulmschneider, D.; Goubeau, J. *Chem. Ber.* **1957**, *90*, 2733−2738.
(15) Pailer, M.; Huemer, H. *Monatsh. Chem.* **1964**, *95*, 373−378.
(16) Dornow, A.; Fischer, K. *Chem. Ber.* **1966**, *99*, 68−71.
(17) Paetzold, P. I.; Stohr, G. *Chem. Ber.* **1968**, *101*, 2874−2880.
(18) Yale, H. L. *J. Heterocycl. Chem.* **1971**, *8*, 205−208.
(19) Goel, A. B.; Gupta, V. D. *J. Organomet. Chem.* **1974**, *77*, 183−188.
(20) Ashe, A. J., III; Fang, X.; Fang, X.; Kampf, J. W. *Organometallics* **2001**, *20*, 5413−5418.
(21) Dürüst, Y.; Dürüst, N.; Akcan, M. *J. Chem. Eng. Data* **2007**, *52*, 718−720.
(22) Dürüst, Y.; Akcan, M.; Martiskainen, O.; Siirola, E.; Pihlaja, K. *Polyhedron* **2008**, *27*, 999−1007.
(23) Weber, L. *Coord. Chem. Rev.* **2008**, *252*, 1−31.
(24) Abbey, E. R.; Zakharov, L. N.; Liu, S.-Y. *J. Am. Chem. Soc.* **2010**, *132*, 16340−16342.
(25) Abbey, E. R.; Zakharov, L. N.; Liu, S.-Y. *J. Am. Chem. Soc.* **2011**, *133*, 11508−11511.
(26) Chrostowska, A.; Xu, S.; Mazière, A.; Boknevitz, K.; Li, B.; Abbey, E. R.; Dargelos, A.; Graciaa, A.; Liu, S.-Y. *J. Am. Chem. Soc.* **2014**, *136*, 11813−11820.
(27) Davies, G. H. M.; Molander, G. A. *J. Org. Chem.* **2016**, *81*, 3771−3779.
(28) Paetzold, P. I. *Z. Anorg. Allg. Chem.* **1963**, *326*, 64−69.
(29) Dewar, M. J. S.; Golden, R.; Spanninger, P. A. *J. Am. Chem. Soc.* **1971**, *93*, 3298−3299.
(30) Dewar, M. J. S.; Spanninger, P. A. *Tetrahedron* **1972**, *28*, 959−961.
(31) Zurwerra, D.; Quetglas, V.; Kloer, D. P.; Renold, P.; Pitterna, T. *Org. Lett.* **2015**, *17*, 74−77.
(32) Lu, W.; Hu, H.; Li, Y.; Ganguly, R.; Kinjo, R. *J. Am. Chem. Soc.* **2016**, *138*, 6650−6661.
(33) Loh, Y. K.; Chong, C. C.; Ganguly, R.; Li, Y.; Vidovic, D.; Kinjo, R. *Chem. Commun.* **2014**, *50*, 8561−8564.
(34) Adachi, S.; Liew, S. K.; Lee, C. F.; Lough, A.; He, Z.; St. Denis, J. D.; Poda, G.; Yudin, A. K. *Org. Lett.* **2015**, *17*, 5594−5597.
(35) Weber, L.; Schnieder, M.; Stammler, H.-G.; Neumann, B.; Schoeller, W. W. *Eur. J. Inorg. Chem.* **1999**, *1999*, 1193−1198.
(36) Chang, M.-C.; Otten, E. *Organometallics* **2016**, *35*, 534−542.
(37) Avramenko, G. V.; Bezuglaya, Z. V.; Stepanov, B. I.; Troitskaya, V. S.; Vinokurov, V. G. *J. Appl. Spectrosc.* **1988**, *48*, 620−624.
(38) *Bioactive Heterocyclic Compound Classes, Agrochemicals and Pharamceuticals*; Lamberth, C., Dinges, J., Eds.; Wiley-VCH: Weinheim, 2012.
(39) Kreuer, K. D.; Fuchs, A.; Ise, M.; Spaeth, M.; Maier, J. *Electrochim. Acta* **1998**, *43*, 1281−1288.
(40) Taydakov, I. V.; Akkuzina, A. A.; Avetisov, R. I.; Khomyakov, A. V.; Saifutyarov, R. R.; Avetissov, I. C. *J. Lumin.* **2016**, *177*, 31−39.
(41) Handa, N. V.; Li, S.; Gerbec, J. A.; Sumitani, N.; Hawker, C. J.; Klinger, D. *J. Am. Chem. Soc.* **2016**, *138*, 6400−6403.
(42) Liu, X.; Zhang, Y.; Li, B.; Zakharov, L. N.; Vasiliu, M.; Dixon, D. A.; Liu, S.-Y. *Angew. Chem., Int. Ed.* **2016**, *55*, 8333−8337.
(43) Hatakeyama, T.; Hashimoto, S.; Seki, S.; Nakamura, M. *J. Am. Chem. Soc.* **2011**, *133*, 18614−18617.
(44) Paulvannan, K.; Hale, R.; Sedehi, D.; Chen, T. *Tetrahedron* **2001**, *57*, 9677−9682.

(45) Ahmed, S.; Longchar, M.; Boruah, R. C. *Indian J. Chem. Sec. B* **1999**, *38*, 125−127.

(46) Li, J.; Neuville, L. *Org. Lett.* **2013**, *15*, 1752−1755.

(47) Crouch, R. D.; Howard, J. L.; Zile, J. L.; Barker, K. H. *J. Chem. Educ.* **2006**, *83*, 1658−1660.

(48) Buck, C.; Gramlich, B.; Wagner, S. 2015, arXiv:150902327v1. arXiv.org e-Print archive (Accessed May 28, 2016). https://arxiv.org/abs/1509.02327v1.

(49) Fery-Forgues, S.; Lavabre, D. *J. Chem. Educ.* **1999**, *76*, 1260−1264.

(50) Consistent with literature value of Lophine **5** ($\Phi_F = 0.27$): Fridman, N.; Kaftory, M.; Speiser, S. *Sens. Actuators B* **2007**, *126*, 107−115.

(51) Frisch, M. J.; Trucks, G. W.; Schlegel, H. B.; Scuseria, G. E.; Robb, M. A.; Cheeseman, J. R.; Scalmani, G.; Barone, V.; Mennucci, B.; Petersson, G. A.; Nakatsuji, H.; Caricato, M.; Li, X.; Hratchian, H. P.; Izmaylov, A. F.; Bloino, J.; Zheng, G.; Sonnenberg, J. L.; Hada, M.; Ehara, M.; Toyota, K.; Fukuda, R.; Hasegawa, J.; Ishida, M.; Nakajima, T.; Honda, Y.; Kitao, O.; Nakai, H.; Vreven, T.; Montgomery, J. A., Jr; Peralta, J. E.; Ogliaro, F.; Bearpark, M.; Heyd, J. J.; Brothers, E.; Kudin, K. N.; Staroverov, V. N.; Kobayashi, R.; Normand, J.; Raghavachari, K.; Rendell, A.; Burant, J. C.; Iyengar, S. S.; Tomasi, J.; Cossi, M.; Rega, N.; Millam, J. M.; Klene, M.; Knox, J. E.; Cross, J. B.; Bakken, V.; Adamo, C.; Jaramillo, J.; Gomperts, R.; Stratmann, R. E.; Yazyev, O.; Austin, A. J.; Cammi, R.; Pomelli, C.; Ochterski, J. W.; Martin, R. L.; Morokuma, K.; Zakrzewski, V. G.; Voth, G. A.; Salvador, P.; Dannenberg, J. J.; Dapprich, S.; Daniels, A. D.; Farkas, O.; Foresman, J. B.; Ortiz, J. V.; Cioslowski, J.; Fox, D. J. *Gaussian 09*, revision D.01; Gaussian, Inc.: Wallingford, CT, 2009.

(52) Chen, Z.; Wannere, C. S.; Corminboeuf, C.; Puchta, R.; Schleyer, P. V. R. *Chem. Rev.* **2005**, *105*, 3842−3888.

(53) We did not follow up with attempts to attain X-ray data for compound **12** in its pure form as we still obtained the pertinent structural data. The reaction was repeated with a longer reaction time followed by recrystallization for full characterization and used for subsequent analyses.

(54) Wu, Y.-Y.; Chen, Y.; Gou, G.-Z.; Mu, W.-H.; Lv, X.-J.; Du, M.-L.; Fu, W.-F. *Org. Lett.* **2012**, *14*, 5226−5229.

(55) Gibson, G. L.; McCormick, T. M.; Seferos, D. S. *J. Am. Chem. Soc.* **2012**, *134*, 539−547.

(56) Gibson, G. L.; McCormick, T. M.; Seferos, D. S. *J. Phys. Chem. C* **2013**, *117*, 16606−16615.

(57) Taniguchi, T.; Yamaguchi, S. *Organometallics* **2010**, *29*, 5732−5735.

(58) Abbey, E. R.; Zakharov, L. N.; Liu, S.-Y. *J. Am. Chem. Soc.* **2008**, *130*, 7250−7252.

(59) Sasaki, S.; Drummen, G. P. C.; Konishi, G.-I. *J. Mater. Chem. C* **2016**, *4*, 2731−2743.

(60) O'Brien, M.; Koos, P.; Browne, D. L.; Ley, S. V. *Org. Biomol. Chem.* **2012**, *10*, 7031−7036.

(61) Sibi, M. P.; Stanley, L. M.; Soeta, T. *Adv. Synth. Catal.* **2006**, *348*, 2371−2375.

(62) Paulvannan, K.; Chen, T.; Hale, R. *Tetrahedron* **2000**, *56*, 8071−8076.

(63) Zhang, T.; Bao, W. *J. Org. Chem.* **2013**, *78*, 1317−1322.

(64) Chen, C.-Y.; Hu, W.-P.; Yan, P.-C.; Senadi, G. C.; Wang, J.-J. *Org. Lett.* **2013**, *15*, 6116−6119.

(65) Chaur, M. N.; Collado, D.; Lehn, J.-M. *Chem. - Eur. J.* **2011**, *17*, 248−258.